ICAS 2016
30th Congress of the International Council of the Aeronautical Sciences
DCC, Daejeon, Korea ; September 25-30, 2016

FLIGHT CONTROL LAW CLEARANCE USING WORST-CASE INPUTS

J. Diepolder, A. Gabrys, S. Schatz, M. Bittner, M. Rieck, B. Grüter, F. Holzapfel,
Institute of Flight System Dynamics, Technische Universität München, Germany

Joseph Z. Ben-Asher,
Faculty of Aerospace Engineering, Technion Institute of Technology Haifa, Israel

Keywords: Control Law Clearance, Trajectory Optimization, Optimal Control.

Abstract

This study explores the effectiveness of applying optimal control techniques to the flight control law clearance problem, which is the challenge of ensuring the safety of an aircraft's flight control system for all allowable inputs. The main criteria chosen were the angle-of-attack limit exceeding criterion in the longitudinal plane, and the angle-of-sideslip limit exceeding criterion in the lateral plane. Other criteria, such as load factor and side-force were also considered. Using general double-engine airplane aero data to obtain realistic aerodynamic coefficients, longitudinal and lateral linear models were developed. The flight control system developed for this aircraft by the Institute of Flight System Dynamics (FSD) of Technische Universität München was used for the clearance task. A linear system of this type has a bang-bang worst case input (i.e. using only maximum or minimum values) when the states are unbounded; but a possible bang-singular-bang or bang-bang-singular worst-case input when one or more states are bounded (i.e. intermediate values are also used). These results were validated with collocation-based optimization using Falcon.m (FSD Optimal Control Tool for MATLAB). In the physical domain these results translate into actuator rate limiting issues; thus limited elevator/rudder/aileron deflection and rate of elevator/rudder/aileron can lead to even more extreme worst case performance. The input signals in this study were pilot commands (stick and pedal) and/or wind disturbances in the form of gusts. The main findings in the longitudinal plane were that the pilot stick commands typically involve maximal/minimal and sometimes intermediate values (whenever the elevator gets saturated). Wind disturbances in this plane (normal gusts) are typically maximal/minimal (bang-bang) and their effect on the aerodynamic angle-of-attack highly depends on the gust shape (equivalent time constant). The main findings in the lateral plane were that the pilot stick commands have very little effect on the sideslip, thus demonstrating a very good decoupling. The pilot pedals, on the other hand, were very effective in building up sideslips and the worst-case structure was obtained by using them periodically (in a trapezoidal wave shape) at the Dutch-roll frequency. The worst-case wind disturbances are non-periodic maximal/minimal (bang-bang) and their effect on the aerodynamic angle-of-sideslip highly depends on the gust shape.

1 Introduction

Flight control law clearance is the practice of ensuring the safety of an aircraft for all admissible time-varying pilot inputs under all possible operational conditions [1]. This procedure is performed before an aircraft is tested in flight, regardless of how stable or robust its control law is designed to be. In theory, in order to clear a flight control law, it must be proven for all variables and uncertainties, over the entire flight envelope, that the aircraft cannot be driven to an uncontrollable state. To date, the practice used in industry is to divide the parameter space into a grid and test the flight control law for a finite number of maneuvers [2].

Unfortunately this method is rather time consuming, costly and by no means foolproof. An alternative approach is optimization; instead of showing that a flight control law is valid under all possible conditions, the worst possible aircraft behaviour is sought, and if it can be demonstrated that the behaviour is within acceptable limits, then the flight control law is valid [3]. For example, when clearing the nonlinear handling criteria of angle-of-attack (AoA) limit exceeding, one would determine a function for AoA (derived from the numerical integration of the chosen model over the specified time interval) which would depend on some uncertain parameters (such as center of gravity along x-axis, y-body-axis moment of inertia, pitching moment coefficient derivatives, etc.)[4]. Then the chosen optimization algorithm would attempt to find the maximum value attained by the AoA by varying these parameters, and if that value does not exceed the maximum permissible AoA then the criterion is cleared. A number of studies have already tried (with some degree of success) to utilize this method with various optimization techniques, such as genetic algorithms, differential evolution and adaptive simulated annealing [1][5][6][7]. However these techniques essentially use brute force to find a solution and tend to be very computationally intensive. Optimal control relies more on the knowledge of the dynamics of the system and will provide accurate quantitative results as well as useful insights.

In [8] the optimal control theory was employed, by direct and indirect methods, in order to improve the means of ensuring flight control clearance. The problem was formulated with a running cost which approximated the maximal AoA over a given time, or a terminal cost of maximal AoA at an arbitrary time. The analysis was based on the Minimum Principle and the characteristics of the worst case control were explored.

The present paper continues to explore the effectiveness of applying optimal control techniques to the flight control law clearance problem. More general linear models are used (instead of the Short-Period approximation in [8]) for the longitudinal as well as the lateral planes, including the effects of wind gusts. The specific criteria chosen were the angle-of-attack (AoA) limit exceeding criterion in the longitudinal plane, and the angle-of-sideslip (AoS) limit exceeding criterion in the lateral plane. Based on direct and indirect methods, the characteristics of the worst case controls and worst case gusts for a general double-engine airplane were explored.

2 Modeling

The model used for the analysis consists of a plant, which includes the aircraft dynamics, a controller, and a servomechanism. The input comes from the pilot commands subject to saturation with predefined bounds and gain. Wind disturbances in the form of gusts are included. Fig. 1 depicts a block diagram of the basic layout.

2.1 Linear Plant Model

In determining the plant we assume the standard linear model which separates the longitudinal and the lateral planes [9]. For the longitudinal plane, after linearization in a straight and level flight at altitude h and velocity V,

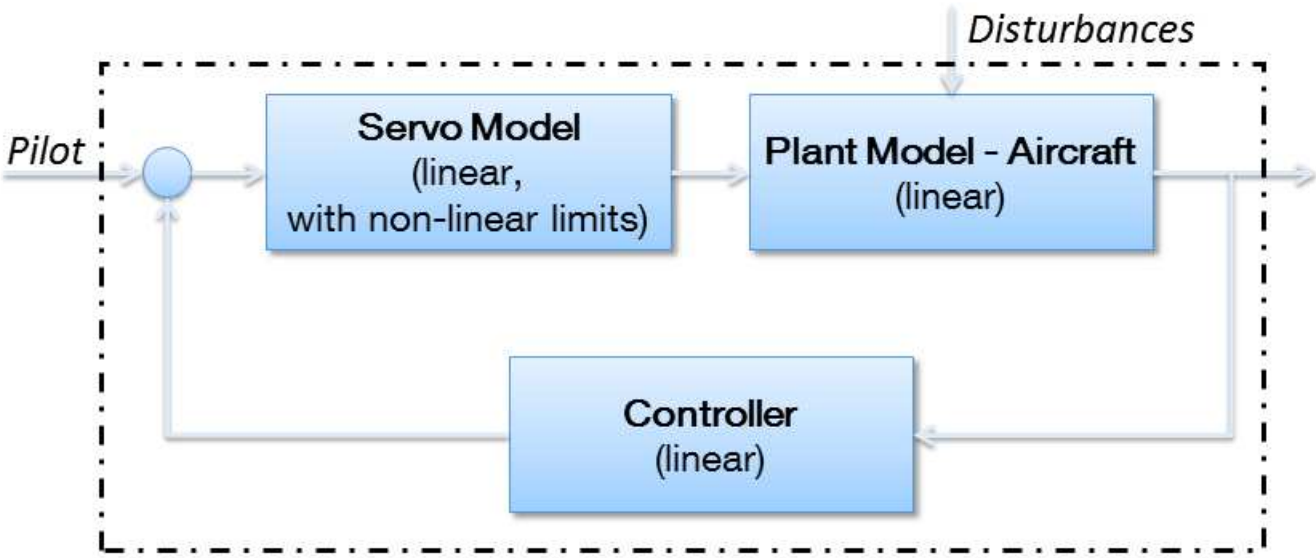

Fig. 1 Basic block diagram of the model.

we obtain:

$$\frac{d}{dt}\begin{bmatrix} u \\ \alpha \\ \theta \\ q \end{bmatrix} = A_{long} \cdot \begin{bmatrix} u \\ \alpha \\ \theta \\ q \end{bmatrix} + B_{long} \cdot \delta_e + [B_w B_{\dot{w}}] \cdot \begin{bmatrix} w_g \\ \dot{w}_g \end{bmatrix} \tag{1}$$

where u is the velocity along x-axis; α is the angle-of-attack; θ is the pitch angle; q is the pitch rate; δ_e is the elevator deflection; and w_g is the vertical gust. For the lateral plane we have:

$$\frac{d}{dt}\begin{bmatrix} r \\ \beta \\ p \\ \phi \end{bmatrix} = A_{lat} \cdot \begin{bmatrix} r \\ \beta \\ p \\ \phi \end{bmatrix} + B_{lat} \cdot \begin{bmatrix} \delta_a \\ \delta_r \end{bmatrix} + [B_v B_{\dot{v}}] \cdot \begin{bmatrix} v_g \\ \dot{v}_g \end{bmatrix} \tag{2}$$

where r is the yaw rate; β is the angle-of-sideslip; p is the roll rate; ϕ is the roll angle; δ_a is the ailron deflection; δ_r is the rudder deflection; and v_g is the lateral gust. The gust values are shaped by a first order filter with a parameter τ:

$$G(s) = \frac{w_g(s)}{w_{g_c}(s)} = \frac{v_g(s)}{v_{g_c}(s)} = \frac{1}{s\tau + 1} \tag{3}$$

where w_{g_c} and v_{g_c} are control-like variables and are arbitrary functions subject to hard-limits. Note that this approximation for the gust enables the search for worst-case gusts in the form of the optimal control theory for linear systems. This would not be the case with fixe-shaped gust. Fig. 2 presents a common fixed-shaped gust using the $\frac{w_g}{2} \cdot (1 - cos(\frac{x\pi}{l}))$ formula [10] (with $x = Vt$ and l being a typical length). The two shapes are somewhat different, however there is no strong reason to prefer one over the other as they are both approximations. Anyway they yield similar results in the simulations.

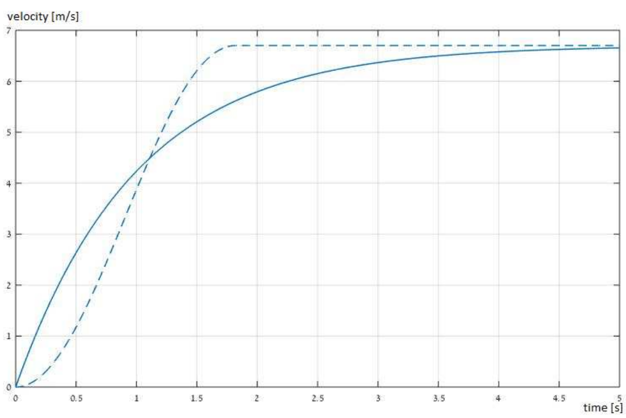

Fig. 2 Gust profile linear (solid) vs. cosine shaped (dashed).

2.2 Servomechanics

A second order servomechanism model with a natural frequency of 40 radians per second and a damping ration of 0.707 was used for all servos:

$$G(s) = \frac{\delta_i}{\delta_{i_c}} = \frac{\omega_n^2}{s^2 + 2\xi\omega_n s + \omega_n^2} = \frac{1600}{s^2 + 56.56s + 1600} \quad (4)$$

where $i \in \{e, a, r\}$, and the sub-index c indicates a commanded value. The control deflections are subject to hard limits as are the angular rates-of-change of the control deflections.

2.3 Control Loops

The flight control system developed for this aircraft by the Institute of Flight System Dynamics of Technische Universität München was used for the clearance task. In the longitudinal plane, the stick force is translated into a normal load command. The control loop includes proportional gains plus an integral term, integrating the error between that actual and the commanded load factor. In the lateral loop the pedal movement is translated into a side-load command whereas the lateral stick-force is translated into a roll angle command. The control loop includes proportional gains plus two integral terms, integrating the errors between that actual and the commanded values. Fig. 3 and Fig. 4 present step commands at a typical envelope point ($h = 2000m$, $V = 55\frac{m}{s}$) for the pitch and yaw control loops. Notice the relatively lower damping of the later with respect to the former. This fact plays a great deal in the following results.

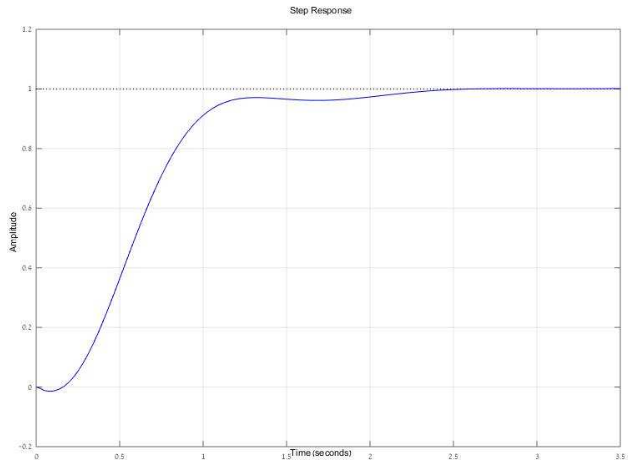

Fig. 3 Step-response in the pitch loop.

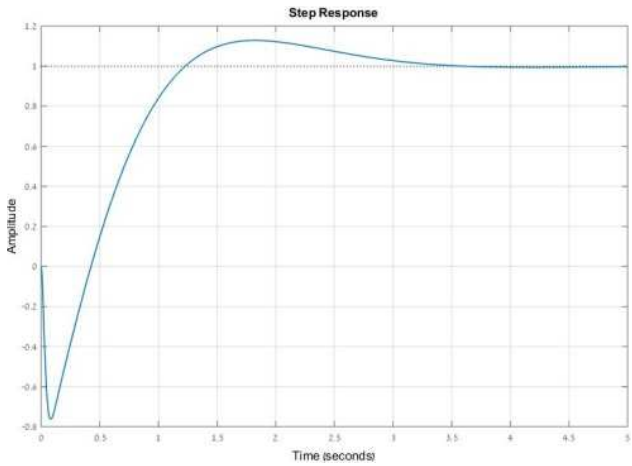

Fig. 4 Step-response in the yaw loop.

3 Problem Formulation

An optimal control problem consists of a cost function, a dynamic system, boundary conditions and sometimes constraints. The dynamic system(s) was covered in the previous section. As for boundary conditions, the focus will only be on initial conditions, specifically $\mathbf{x}(t_0) = 0$ which translates into straight and level flight. The main step now is turning the clearance criterion into an appropriate cost function. The clearance criteria which were the focus of this project were the angle-of-attack limit exceeding criterion in the longitudinal plane and the angle-of-sideslip limit exceeding criterion in the lateral plane. Increasing the angle-of-attack (AoA) is generally associated with increasing the lift force, however after reaching the critical angle, which produces the maximum lift, further growth results in a stall. Therefore it is in the interest of the control engineer to ensure that aircraft cannot increase its angle-of-attack beyond the critical angle. Similar considerations apply to the angle of sideslip (AoS) in the lateral plane. Thinking about this in terms of optimization, these criteria can be expressed as follows: If the maximum AoA/AoS produced by the worst case pilot input (and/or the worst case gust values) is less than the critical angle (or some smaller angle if a factor of safety is included) then the criterion is satisfied. This means that the cost function must be structured in such a way that it maximizes the largest possible magnitude of AoA/AoS within the chosen time interval. The cost function is described as follows: maximize the magnitude of the AoA/AoS at an unspecified final time t_f. This form is easily described with a Mayer formulation, and by keeping t_f free it allows the optimization tool to choose the proper final time such that the maximum magnitude is achieved. Constraints are useful for describing the physical limitations of the systems. The control surfaces of an aircraft cannot move a full 360° at infinite speeds. They have maximum and minimum displacements as well as maximum angular speeds. If the displacement or angular speed of a control surface is described by a state (using (4)), these bounds are easily incorporated into the system in terms of state constraints.

4 Theoretical Analysis

4.1 Unbounded Case

Claim: For a single-input LTI system with the form:

$$\dot{\mathbf{x}} = \mathbf{A}\mathbf{x} + \mathbf{B}u \tag{5}$$

$$\mathbf{y} = \mathbf{C}\mathbf{x} \tag{6}$$

$$\begin{gathered} \mathbf{x} \in \mathbb{R}^n, u \in \mathbb{R}, \mathbf{y} \in \mathbb{R}^m \\ \mathbf{A} \in \mathbb{R}^{nxn}, \mathbf{B} \in \mathbb{R}^{nx1}, \mathbf{C} \in \mathbb{R}^{1xn} \end{gathered} \tag{7}$$

$$u_{min} \leq u \leq u_{max} \tag{8}$$

$$\mathbf{x}(t_0) = \mathbf{x}_0 \tag{9}$$

Subject to the cost function:

$$\min\left(y\left(t_f\right)\right) \tag{10}$$

The optimal control is bang-bang.
Remarks:

- The final time t_f is free but is typically subject to an upper limit i.e $t_f \leq t_{f_M}$
- The same proof with opposite signs holds for $\max\left(y\left(t_f\right)\right)$

Proof:

$$H\left(\mathbf{x}, u, t, \boldsymbol{\lambda}\right) = \boldsymbol{\lambda}^T\left(\mathbf{A}\mathbf{x} + \mathbf{B}u\right) \tag{11}$$

Using Pontryagin's Minimum Principle [22]:

$$\dot{\boldsymbol{\lambda}} = -\frac{\partial H}{\partial \mathbf{x}} = -\mathbf{A}^T\boldsymbol{\lambda} \tag{12}$$

$$\bar{u} = arg\min_u H\left(\mathbf{x}, u, t, \boldsymbol{\lambda}\right) = \begin{cases} u_{max}, \boldsymbol{\lambda}^T\mathbf{B} < 0 \\ u_{min}, \boldsymbol{\lambda}^T\mathbf{B} > 0 \\ u_{sing}, \boldsymbol{\lambda}^T\mathbf{B} = 0 \end{cases} \tag{13}$$

$$u_{sing} \in \left[u_{min}, u_{max}\right] \tag{14}$$

Therefore the solution is either bang-bang, or bang-singular-bang, with a switching function that is a linear combination of the costates.

To determine the singular control, the time derivatives of H_u must be equal to zero. From this result it can be shown that:

$$\mathbf{B}^T\left(\mathbf{A}^k\right)^T\boldsymbol{\lambda} = 0, k = 0, 1, 2, ... \tag{15}$$

If the system is controllable, the only λ that satisfies them is the trivial solution.

$$\begin{bmatrix} \mathbf{B}^T \\ \mathbf{B}^T\mathbf{A}^T \\ \vdots \\ \mathbf{B}^T\left(\mathbf{A}^{n-1}\right)^T \end{bmatrix} \boldsymbol{\lambda} = 0 \tag{16}$$

$$\mathbf{C}^T\boldsymbol{\lambda} = 0 \tag{17}$$

Where $\mathbf{C}$ is the controllability matrix of the system. If the system is controllable, then $\mathbf{C}$ is full rank (and invertible):

$$\left(\mathbf{C}^T\right)^{-1}\mathbf{C}^T\boldsymbol{\lambda} = \left(\mathbf{C}^T\right)^{-1}0 \tag{18}$$

$$\boldsymbol{\lambda} = 0 \tag{19}$$

A singular solution only exists when each element of $\boldsymbol{\lambda}$ remains zero for a non-instantaneous time interval. This contradicts the minimum principle, thus the solution which results in the maximum J is non-singular, bang-bang.

Remarks:

- The above is the standard procedure for the non-singularity of linear time-optimal problems.
- For more than one control, i.e. $\mathbf{u} \in \mathbb{R}^k$, if the system is controllable with respect to each controller, then we will not have a singular arc. The proof for that is similar to the above.

4.2 Bounded Case

Next, consider state bounds, which can be expressed as inequality constraints on the state variables. (Note: For multiple constraints just repeat this process with a new additional S and μ, and the solution will be of a similar form):

Claim: For the single-input LTI system (5)-(10) with the additional constraint imposed on state i:

$$|x_i| \leq x_{i_{max}} \tag{20}$$

Or, equivalently

$$S(\mathbf{x}, t) = x_i^2 - (x_{i_{max}})^2 \leq 0 \tag{21}$$

The optimal control is bang-bang with (possible) singular arcs.

Remark: We call it "singular" because of the way the Hamiltonian is going to be defined (22). In fact this is simply the control as determined by the equality constraint - see below - typically with intermediate values with respect to the control bounds.

Proof: The Hamiltonian is extended to include the state constraints, as follows:

$$H = \boldsymbol{\lambda}^T (\mathbf{A}\mathbf{x} + \mathbf{B}u) + \mu \left(x_i^2 - x_{i_{max}}^2 \right) \tag{22}$$

Where

$$\mu = \begin{cases} = 0, S < 0 \\ > 0, S = 0 \end{cases} \tag{23}$$

The Euler-Lagrange equations become:

$$\dot{\boldsymbol{\lambda}} = -\frac{\partial H}{\partial \mathbf{x}} = -\mathbf{A}^T \boldsymbol{\lambda} - \mu \begin{bmatrix} 0 \\ \vdots \\ 2x_i \\ \vdots \\ 0 \end{bmatrix} \tag{24}$$

And the optimal control is:

$$\bar{u} = arg \min_u H(\mathbf{x}, u, t, \boldsymbol{\lambda}) = \begin{cases} u_{max}, \boldsymbol{\lambda}^T \mathbf{B} < 0 \\ u_{min}, \boldsymbol{\lambda}^T \mathbf{B} > 0 \\ u_{sing}, \boldsymbol{\lambda}^T \mathbf{B} = 0 \end{cases} \tag{25}$$

The singular optimal control can be determined from $S = 0$ as:

$$\dot{x}_i = e_i A x + b_i u = 0 \rightarrow u_{sing} = -\frac{e_i A x}{b_i} \tag{26}$$

Where e_i is the row vector of size n with the only non-zero entry being 1 at index i. Finally, by equating the second time derivative of $H_u = \mathbf{B}^T \boldsymbol{\lambda}$ to 0, we get:

$$-\mathbf{B}^T \mathbf{A}^T \dot{\boldsymbol{\lambda}} - 2\mu \dot{x}_i b_i - 2\dot{\mu} x_i b_i = 0 \tag{27}$$

$$-\mathbf{B}^T \left(\mathbf{A}^2 \right)^T \boldsymbol{\lambda} - 2\mu x_i \mathbf{B}^T \mathbf{A}^T \mathbf{e_i}^T - 2\dot{\mu} x_i b_i = 0 \tag{28}$$

From (28) we readily obtain the differential equation governing μ.

5 Longitudinal Optimization Results - Maximizing AoA

The following example for the longitudinal plane is aimed at maximizing the aerodynamic AoA for a combined stick and wind input. The wind time constant is $\tau = 1s$ and its maximum value $6.7\frac{m}{s}$. The nominal flight speed is $55\frac{m}{s}$ and the time horizon is set to $8.5s$. Notice that the linearization validity over such a long, strong maneuver deteriorates and the results can no longer be considered quantitatively.

Fig. 5 presents the worst-case results. For the time horizon in this example the servo limits are reached as can be seen in Fig. 5 and the worst-case stick input comprises bang-bang and singular arcs. Note that the

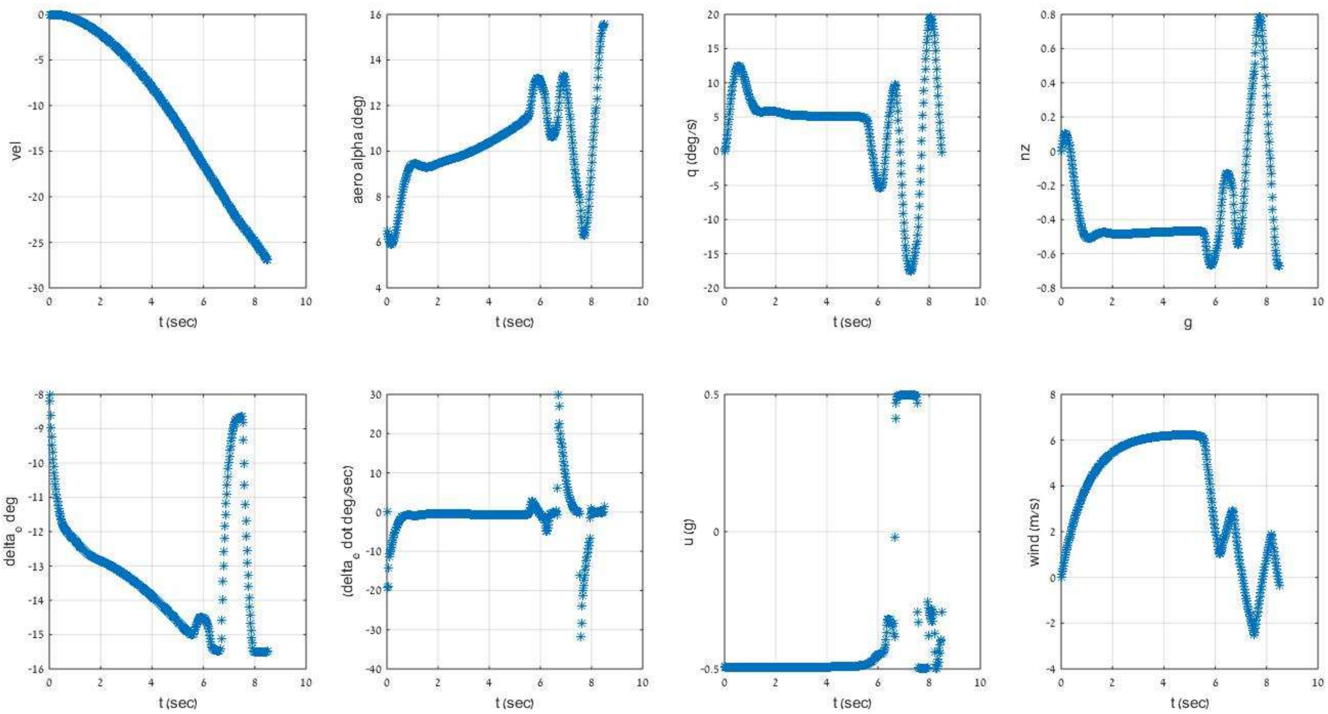

Fig. 5 Responses for worst-case stick and wind inputs (maximizing AoA)

inclusion of bounds slows down the system and decreases the maximum AoA which could be reached without considering the respective limits. The corresponding switching function $\boldsymbol{\lambda}^{\boldsymbol{T}}\boldsymbol{B}$ is shown in Fig. 6 and it satisfies (25).

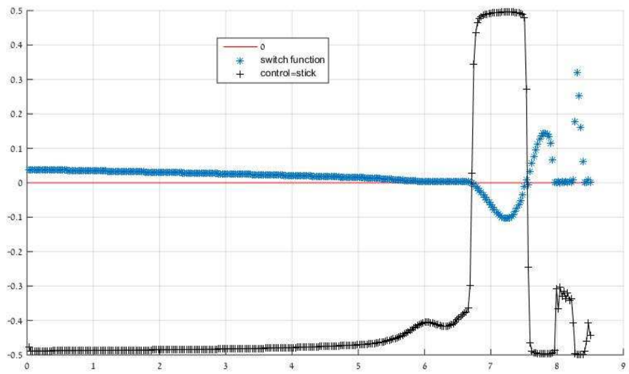

Fig. 6 Switching structure for worst-case stick and wind inputs (maximizing AoA)

6 Lateral Optimization Results - Maximizing AoS

For the lateral plane the objective is to maximize the aerodynamic AoS. First we will only use the pedal command without wind input. Furthermore the lateral stick command is not used here as it does not change the results significantly thus demonstrating a very nice roll-yaw decoupling of the control laws. Again the nominal flight speed is $55\frac{m}{s}$ and the maximum time horizon is now set to $10s$. The resulting responses are shown in Fig. 7. The pedal command δ_r is bang-singular-bang and corresponds very nicely with the Dutch-Roll frequency $(1.3\frac{rad}{s} = 0.2Hz)$ over the entire allowable $10s$. The switching function is plotted in Fig. 8, and it satisfies (25).

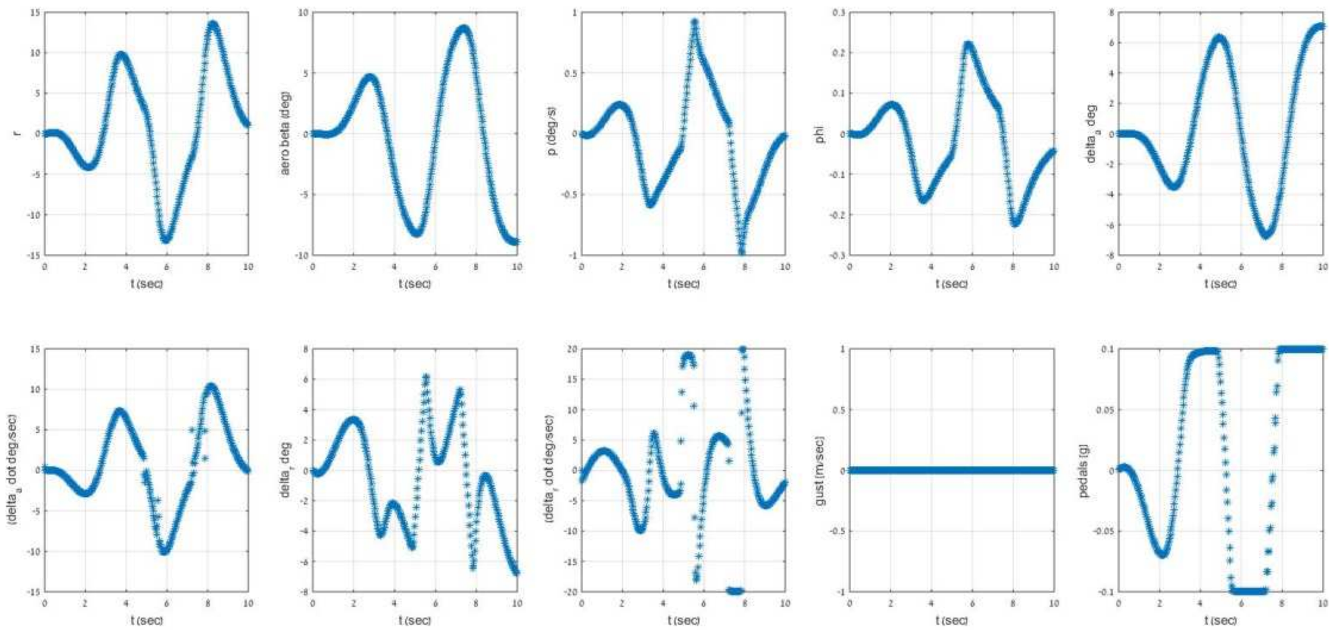

Fig. 7 Responses for worst-case pedal inputs (maximizing AoS)

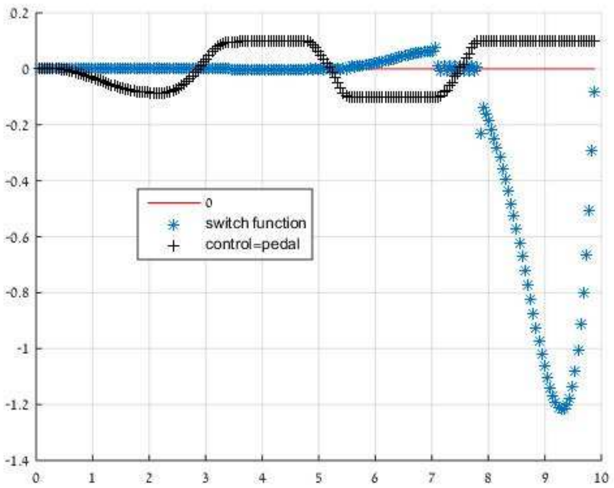

Fig. 8 Switching structure for worst-case pedal inputs (maximizing AoS)

Finally the combined worst-case scenario for pedal inputs with gusts of $\tau = 2s$ are presented in Fig. 9. Please note that again the servo bounds have been reached. As can be expected, the combined response (Fig. 9) leads to a further increase for the aerodynamic AoS at the end of the time horizon compared to the previous case (Fig. 7).

7 Conclusions

The most important result of this work is the validation that the clearance problem (specifically, the AoA, AoS limit-exceeding criteria) can be framed and solved as an optimal control problem. This allows for the problem to be solved in a format that is more familiar to control engineers, with available software and optimization tools. This can drastically help to reduce the overhead in time to learn and implement the procedure. The theoretical analysis proved that, for the linear system, the worst case input is bang-bang with costate-dependent switching function when the states are unbounded and the system is completely controllable, and is possibly bang-singular-bang otherwise. When solved numerically the optimization results, matched perfectly with the theoretical analysis. They have also been in fair agreement with the 6DOF results when the validity of the linearization was maintained. The results can be used a starting point for a more intensive 6DOF Monte-Carlo study. This study will be based on the obtained worst-case control / disturbance structures, and will incorporate a sensitivity study to all relevant parameters in order to validate

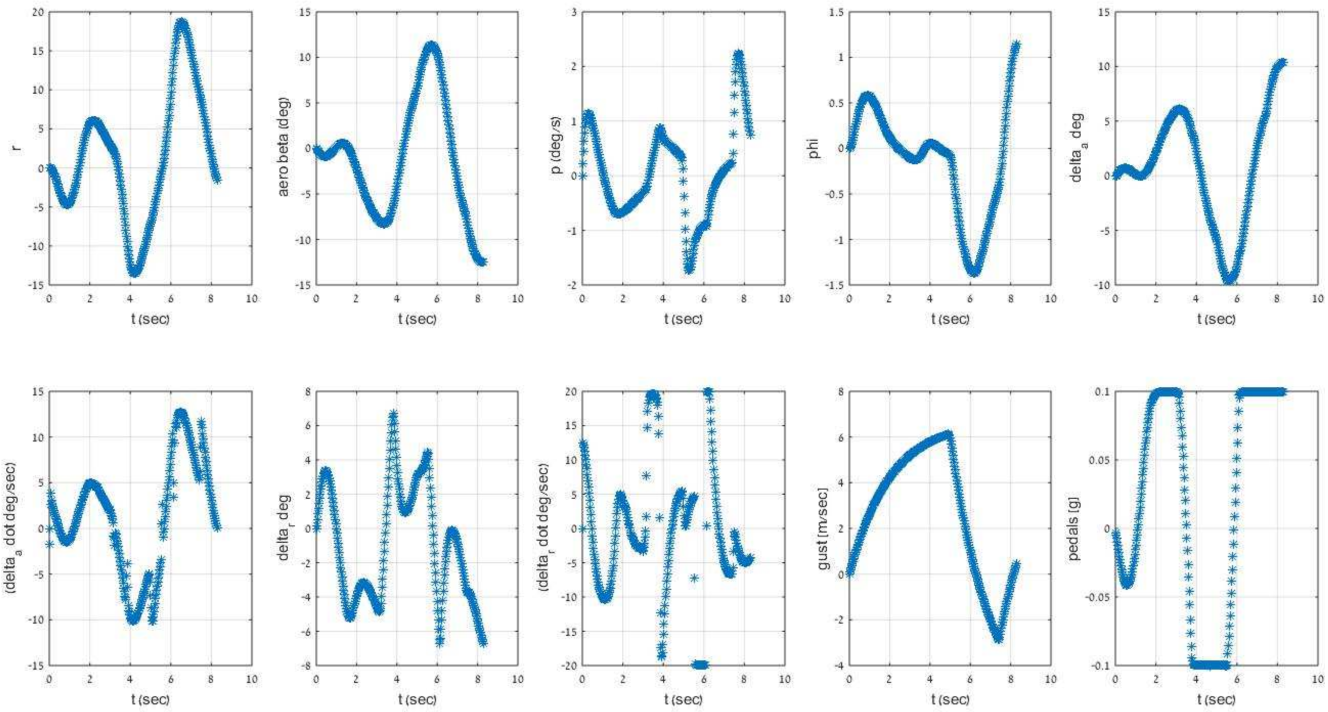

Fig. 9 Responses for worst-case pedal and wind inputs (maximizing AoS)

the flight control systems. The optimization with a non-linear 6DOF model seems like a feasible task with the available software tools (like *FALCON.m* or GPOPS), and it is recommended for further research.

8 Contact Author Email Address

Johannes.Diepolder@tum.de

Acknowledgments

The authors wish to thank Avriel Herrmann of Rafael for editing the paper and for his useful comments. This work was supported by the DFG grant HO4190/8-1.

Copyright Statement

References

[1] Joos, H. D., "Flight Control Law Clearance Using Optimization-Based Worst-Case Search", Proceedings of the *6th International Federation of Automatic Control Symposium on Robust Control Design*, Haifa, Israel, June 2009.

[2] Hanson, A., "Clearance of Flight Control Laws Using Optimization", AST5-CT-2006-030768, January 2010.

[3] Kos, J., and ten Dam, A. A., "Optimization Problems, Methods and Techniques in Flight Control Design", *Group for Aeronautical Research and Technology in Europe*, TP-100-2, Netherlands, May 1997.

[4] Fielding, C., Varga, A., Bennani, S., and Selier, M., "Advanced Techniques for Clearance of Flight Control Laws", *Lecture Notes in Control and Information Sciences*, Vol. 283, Springer, 2002.

[5] Skoogh, D., Elisasson, P., Berefelt, F., Amiree, R., Tourde, D., and Forssell, L., "Clearance of Flight Control Laws for Time Varying Pilot Input Signals", Proceedings of the *6th International Federation of Automatic Control Symposium on Robust Control Design* , Haifa, Israel, June 2009.

[6] Menon, P. P., Kim, J., Bates, D. G., and Postlethwaite, I., "Clearance of Nonlinear Flight Control Laws Using Hybrid Evolutionary Optimization", *IEEE Transactions on Evolutionary Computation* , Vol. 10, No. 6, December 2006, pp. 689-699.

[7] Forssell, L. S.,and Hyden, A., "Flight Control System Validation Using Global Nonlinear Optimisation Algorithms" *Proceedings of the European Control Conference* , Cambridge, U.K., September 2003.

[8] Herrmann, A. and Ben-Asher, J. Z, Flight Control Law Clearance using Optimal Control Theory, AIAA J. of Aircraft, to appear

[9] Blakelock, J. H., "Automatic Control of Aircraft and Missiles" 2nd Ed., *John Wiley & Sons, Inc.* 1991.

[10] Military Specification MIL-DTL-9490E, 6th April 2008. p. 23.